Available online at www.sciencedirect.com

SciVerse ScienceDirect

Ceramics International 39 (2013) 489–495

CERAMICS INTERNATIONAL

www.elsevier.com/locate/ceramint

Porcelain containing anatase and rutile nanocrystals

N. Bouzidi[a,*], A. Bouzidi[b], P. Gaudon[c], D. Merabet[a], P. Blanchart[d]

[a]*University of Bejaia, Materials Technology Laboratory of Process Engineering (LTMGP). Targua Ouzemmour Road, Bejaia 06000, Algeria*
[b]*University of Bejaia, Electrical Engineering Laboratory (LGE), Targua Ouzemmour Road, Bejaia 06000, Algeria*
[c]*Ecole des Mines d'Alès, Centre des Matériaux de Grande Diffusion (CMGD). 6, Av. de Claviere, 30319 Alés, France*
[d]*GEMH ENSCI, 12 Rue Atlantis, 87068 Limoges, France*

Received 25 May 2012; received in revised form 13 June 2012; accepted 18 June 2012
Available online 1 July 2012

Abstract

The aim of this work is to study the dielectric of two porcelains containing TiO_2 in the form of anatase and rutile. TiO_2 was added in compositions by means of raw kaolin with a relative high quantity of anatase, or the addition of anatase powder (10 wt%) in the initial mixture. An alternative porcelain containing kaolin–anatase mixture was obtained by a preliminary firing at 1300 °C. Beside kaolin, compositions also contain quartz and alkaline feldspar.

The microstructural observations show various crystalline phases and micropores, which also have an effective role in affecting the properties. The dielectric characterization of fired porcelain, in the frequency range of 10^5–10^9 Hz, shows that permittivity value can be increased from 7.19 to 8.41, depending in TiO_2 crystal type, morphology and content. Permittivity depends also on mullite, quartz and cristobalite, quantities, but the role of TiO_2 phase is predominant. The macroscopic permittivity of porcelains can be calculated using a mixing rule, which fit accurately experimental results.

Keywords: C. Dielectric properties; D. Porcelain; Rutile; Anatase

1. Introduction

Kaolins are widely used materials in the ceramic industry and in the manufacture of porcelain for electrotechnical devices, such as high voltage capacitors [1]. Kaolin content in compositions is often up to 50 wt%, but in the form of various mineral phases that contribute to the global material properties [2]. In particular, titanium minerals are mostly from kaolins, and they range from 1.3 wt% to 3.5 wt%. They are mostly in the form of anatase or minor quantities of rutile and brookite [3]. Kaolins containing anatase are widely used in compositions of electrotechnical porcelains since they improve dielectric properties [4,5].

Anatase has a tetragonal structure with irregular octahedra of oxygens, where Ti–O interatomic distances is about 1.917 Å. Rutile structure is different with a tetragonal arrangement of cation and octahedral arrangement of oxygens around cations. Ti–O distances are about 1.959 Å and Ti–Ti bonds are 2.96 Å or 3.57 Å [6]. In general, structural arrangement, cristallinity degree and size of anatase crystals strongly influence permittivity and dielectric loss, in the frequency range considered for dielectric porcelains.

The relative permittivity of anatase phase was reported to be $\varepsilon_r=48$ for powders [7] and $\varepsilon_r=40$ for thin films [8]. Rutile phase was reported to be $\varepsilon_r=89$ along *a*-axis and $\varepsilon_r=173$ along *c*-axis due to its anisotropic nature. A value of $\varepsilon_r=127$ can be considered as an average [9,10]. With powder compacts, the apparent density, grain morphology and thermal treatment change progressively the microcrystal structure, and most effectively at temperature close to that of the anatase–rutile transformation. Particularly, the low frequency (1 kHz) dielectric constant of compressed TiO_2 powder of anatase exceed ($\varepsilon_r=40$–150) that of rutile ($\varepsilon_r=8$–15) [11]. After firing at temperature above 850 °C, the progressive transformation to rutile induces the decrease of ε_r down to 8–15 and a subsequent increase above 1150 °C of $\varepsilon_r=18$–25. Structural transformations are also determinant in dielectric loss, since anatase powder

*Corresponding author. Tel.: +213 793634550.
E-mail address: nedjmabouzidi@yahoo.fr (N. Bouzidi).

0272-8842/$36.00
http://dx.doi.org/10.1016/j.ceramint.2012.06.053

present excessive dielectric loss above 1 kHz. TiO_2 particle sizes also change dielectric constant [12,10] since nanometric grains have a dielectric constant higher than that of coarse grains. The permittivity of nano-rutile exceed that of nano-anatase, above $\varepsilon_r = 100$ in the low frequency range below 10 kHz [11].

During heating in air, the most part of anatase is irreversibly transformed into rutile in 600–700 °C range [13]. Various additives in starting compositions can be added to control the transformation rate of anatase during sintering [14]. In particular, small quantity of tungsten oxide is able to increase the transformation temperature, whereas some oxides such as CuO, CoO and Fe_2O_3 accelerate the transformation rate. In the case of anatase from kaolin, the structural transformation is shifted to higher temperature, since it is in the form of isolated nanometric grains. It is due to the specific nucleation and growth mechanisms of rutile from neighboring grains of anatase [15]. The shift of the in-situ structural transformation of nano-anatase into nano-rutile is favorable to the increase of the macroscopic dielectric properties, since nano rutile have a high permittivity ($\varepsilon_r > 100$).

Porcelains are generally mixtures of ≈ 50 wt% of kaolin and clays, ≈ 30 wt% of flux (feldspar…) and ≈ 20 wt% of quartz. Sintering results in the formation of a composite microstructure with crystals of mullite, relicts of quartz and cristobalite embedded in a glassy matrix [16]. The dielectric properties of porcelain such as dielectric permittivity and the dielectric loss factor depend on the characteristics and relative quantities of different phases [17]. Particularly, cristobalite and quartz phases tend to lower the global dielectric loss, whereas mullite increases dielectric loss. The glassy phase which is derived from feldspar and often contains metal oxide impurities has a very important role since it increases the global conductivity value. Usually, the strength of high voltage insulators is increased by the addition of corundum replacing quartz in starting compositions [18].

The objective of this study is to assess the influence of dispersed TiO_2 crystallites in silico–alumina porcelain. TiO_2 is added by means of a kaolin containing anatase and by means of limited quantity of anatase fine powder. Relative permittivity and dielectric loss were measured in a large frequency range. The role of microstructural characteristics on dielectric properties is analyzed as a function of TiO_2 content and type.

2. Materials and methods

Raw kaolin (KT), from France (Charentes) is used in porcelain compositions in two ways: (a) powder of raw kaolin; (b) chamotte kaolin after mixing with anatase (99.995% purity; *Aldrich Chemical Campany*) and calcinations at 1300 °C, 0.5 h.

Two porcelain types were used: (a) common porcelain, obtained from 50 wt% of kaolin (KT), 30 wt% feldspar and 20 wt% of quartz sand; (b) chamotte porcelain containing chamotte kaolin (50 wt%), that is raw kaolin mixed with anatase and fired at 1300 °C, 0.5 h. The different processing stages of the two porcelain types are summarized in Fig. 1.

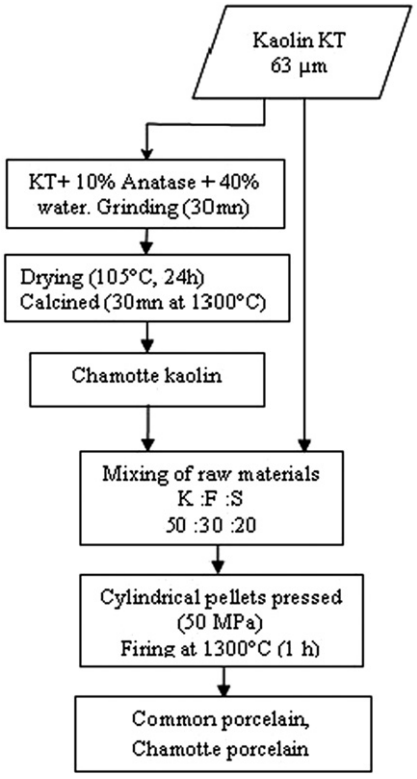

Fig. 1. Processing stages of the two porcelain types.

Heat treatments were made in air atmosphere (Nabertherm electric kiln), up to 1300 °C during 1 h, with heating and cooling ramps of 5 °C min^{-1}. The chemical compositions of phases were determined by X-ray fluorescence (PANalytical Perl'X 3). Mineralogical analyses were made by X-ray diffractometry (Bruker D8; CuK_α, 2–99°2θ, 0.017°2θ step). Quantitative analyses of the different phases were made from XRD diagrams by Rietveld refinements, using NaF as internal standard. The peak height ratio of mullite {1 2 1}, quartz {1 1 2}, cristobalite {1 0 1}, anatase {1 0 1}, rutile {1 1 0} and NaF {200–202} gave the quantity of each phase. The direct calculation of crystallite sizes of {1 0 1} anatase $\beta_{1\,0\,1}$ and {1 1 0} rutile $\beta_{1\,1\,0}$ was performed by the Scherer formula according to Eq. (1):

$$\beta_{1\ 0\ 1} = \beta_{1\ 1\ 0} = k \times \lambda / L \times \cos\theta \quad (1)$$

The amount of amorphous phase was obtained knowing the total quantity of the different crystalline phases. The microstructure, morphology and particle size were observed by Scanning Electron Microscope (FEI Quanta 200 SEM) equipped with a scanning transmission electron microscopy detector (STEM). Surface of samples were polished and chemically etched with HF (40%; 1 min). The determination of bulk densities were achieved by the Archimedes's method in water, and absolute densities were measured by helium pycnometry (Micromeritics AccuPyc).

Bulk and absolute densities were used to calculate the total porosity of samples.

The dielectric properties (relative permittivity ε_r; resistivity R and dielectric loss $\tan\delta$) were determined using complex impedance analyses (HP4291A Hewlett–Packard) in the frequency range of 1 MHz–1 GHz, with thin disks (1 mm) of 10 mm diameter. In the lower frequency range of 1–100 kHz, a different method of impedance analysis was used (Solartron 1260 Impedance Analyzer), with samples of 30 mm diameter. In that case, both sides of samples were polished and coated with a conductive silver paste.

3. Results

The chemical and mineralogical compositions of raw materials are reported in Table 1. Raw KT kaolin contains relatively high quantities of SiO_2 and Al_2O_3, of 42.40 wt% and 37.84 wt%, respectively, and TiO_2 content (1.99 wt%) is relatively high. Kaolinite is the major mineralogical phase seen in XRD of Fig. 2 in raw kaolin. Anatase and a small quantity of rutile are detected at 25.27 and 27.43°2θ, respectively. Weight loss at 1000 °C is of 16.78 wt%, as a consequence of kaolinite dehydroxylation (91 wt% of the structural hydroxyls), but also from gibbsite and organic matter. Alkaline feldspar (orthoclase–albite) and quartz sand (containing small amounts of orthoclase and muscovite) used for porcelain compositions have chemical and mineralogical composition also reported in Table 1.

Fired raw KT kaolin at 1300 °C, 0.5 h reveals the diffraction lines of mullite and cristobalite (Fig. 2), in accordance to the phase diagram SiO_2–Al_2O_3. Fig. 2 presents also the XRD pattern of chamotte kaolin (mixed with 10 wt% of anatase and fired at 1300 °C, 0.5 h), which presents diffraction lines of mullite, cristobalite, and both anatase and rutile phases.

In Fig. 3, the XRD pattern of common porcelain shows peaks of mullite and quartz, but cristobalite and TiO_2 phases are not detected. In the case of chamotte porcelain, the XRD pattern shows the coexistence of mullite, cristobalite, and both anatase and rutile phases.

Table 1
Chemical composition of raw materials.

Oxides (%)	KT	Feldspar	Sand
SiO_2	42.40	74.60	80.98
Al_2O_3	37.84	12.97	11.94
Fe_2O_3	0.55	1.73	0.77
MnO	0.07	0.04	0.00
MgO	0.05	0.41	0.24
CaO	0.26	1.08	0.18
Na_2O	0.03	3.78	0.25
K_2O	0.02	4.64	3.46
TiO_2	1.99	0.00	0.26
P_2O_5	0.00	0.03	0.04
LOI	16.78	0.72	1.88
minéralogy	91% kaolinite, 3% gibbsite, 2% quartz 2% anatase/ rutile, others:2%	Muscovite, quartz, orthose, albite, kaolinite	Quartz, muscovite, orthose

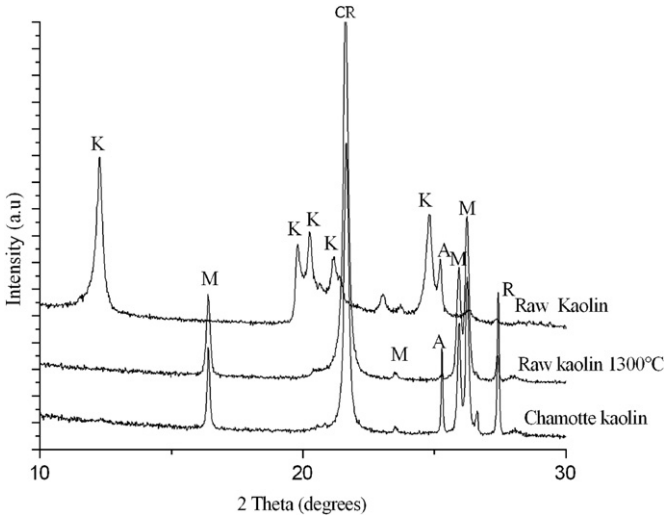

Fig. 2. Diagram of X-ray samples of raw kaolin, raw kaolin fired at 1300 °C and chamotte kaolin (Q: quartz, M: mullite, CR: cristobalite, A: anatase, R: rutile).

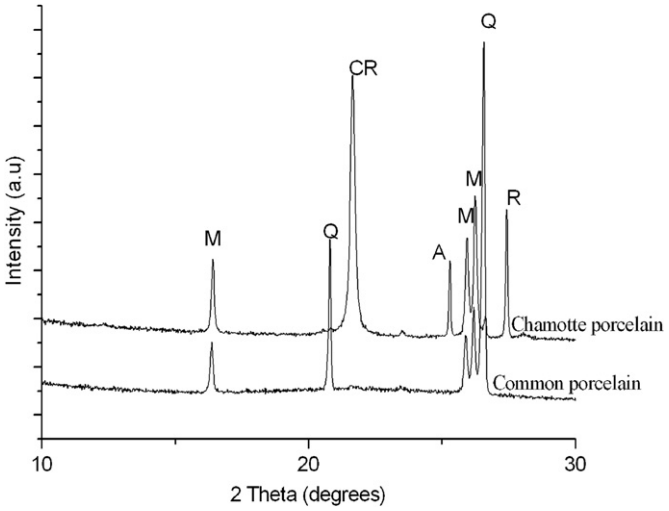

Fig. 3. Diagram of X-ray samples of common porcelain and chamotte porcelain fired at 1300 °C. (Q: quartz, M: mullite, CR: cristobalite, A: anatase, R: rutile).

The quantitative mineralogical analysis of phases formed during the sintering of the two porcelains is reported in Table 2. The most important point is the presence of both anatase and rutile phases in fired chamotte porcelain, but quartz is fully transformed into cristobalite. The crystallite sizes from XRD {1 0 1} peak of anatase and {1 1 0} rutile in raw kaolin, calcined kaolin (1300 °C), and chamotte kaolin are presented in Table 3.

In Fig. 5, porosity measurements as a function of temperature (900–1300 °C) show a significant decrease, to attain 12 vol% and 17 vol% for common porcelain and chamotte porcelain respectively.

Table 2
Quantitative analysis of the main mineralogical phases of porcelains.

Porcelain	Mullite (%)	Quartz (%)	Cristobalite (%)	Rutile (%	Anatase (%)	Glassy phase (%)
Common porcelain	15 ± 1	25 ± 1	0	0	0	60 ± 2
Chamotte porcelain	24 ± 1	0	17 ± 1	4 ± 0.5	3 ± 0.5	52 ± 2

Table 3
Crystallite sizes of anatase {1 0 1} and rutile {1 1 0} in kaolin and porcelain.

β (nm)	Raw kaolin	Calcined kaolin	Chamotte kaolin	Common porcelain	Chamotte porcelain
Anatase	163.33	181.4	242	–	172.3
Rutile	130.4	189.4	228.6	–	223.8

Table 4
Permittivity as a function of frequency of porcelains.

Log F (Hz)	5	7	8	9
Common porcelain	7.19	5.27	5.22	5.12
Chamotte porcelain	8.41	5.33	5.31	5.25

Table 5
Calculated relative bulk permittivity before $_{th}$ and after $_{c}$ correction of porosity.

Log$F$ (Hz)	5			7			8			9		
	$\varepsilon_{\exp}$	ε_c	ε_{th}	ε_{exp}	ε_c	ε_{th}	$\varepsilon_{\exp}$	ε_c	ε_{th}	$\varepsilon_{\exp}$	ε_c	ε_{th}
Common porcelain	7.19	8.03	5.53	5.27	5,82	5.53	5.22	5.79	5.53	5.12	5.68	5.53
Chamotte porcelain	8.41	9.92	8.89	5.33	6.21	8.89	5.31	6.19	8.89	5.25	6.12	8.89

Table 6
Dielectric loss (tang δ) against frequency of porcelains.

Log frequency (Hz)	5	7	8	9
Chamotte porcelain	0.072	0.03	0.03	0.03
Common porcelain	0.045	0.003	0.004	0.005

The relative permittivities of the different samples at an intermediate frequency of 100 kHz are relatively high (Table 4). The common porcelain has a relatively high dielectric permittivity of $\varepsilon_r = 7.19$ in comparison to average value of porcelains ($5 < \varepsilon_r < 6$). For chamotte porcelain the permittivity increase significantly, up to $\varepsilon_r = 8.41$. For both porcelain, permittivity decrease with frequency, but not drastically at the upper bound of the measurement range of 10^9 Hz. Calculation of relative bulk permittivity before (ε_{th}) and after (ε_c) the correction of porosity role are presented in Table 5. The dielectric loss of common and chamotte porcelain as function of frequency are presented in Table 6.

Fig. 4a–c shows the SEM photos of raw kaolin powder, chamotte kaolin powder and chamotte porcelain, respectively. Photo of powders show the crystallite size of initial kaolinite and of heat transformed kaolin and anatase mixture at 1300 °C. The dense microstructure of chamotte porcelain is seen in Fig. 4c, at the interface of the porcelain phase and the chamotte phase. It shows the typical microstructure of porcelain, where remaining crystalline phases are embedded in a glassy matrix [16].

4. Discussion

In X-ray patterns, anatase and rutile main peaks are at diffraction angles of 25.30° and 27.43°2θ for the {1 1 0} reflection. Chamotte porcelain (with 10 wt% of anatase powder added in the starting composition) shows well distinctive rutile peaks and untransformed anatase phase. The most part of rutile crystals seems to not enter into the glassy phase. This is probably due to the important

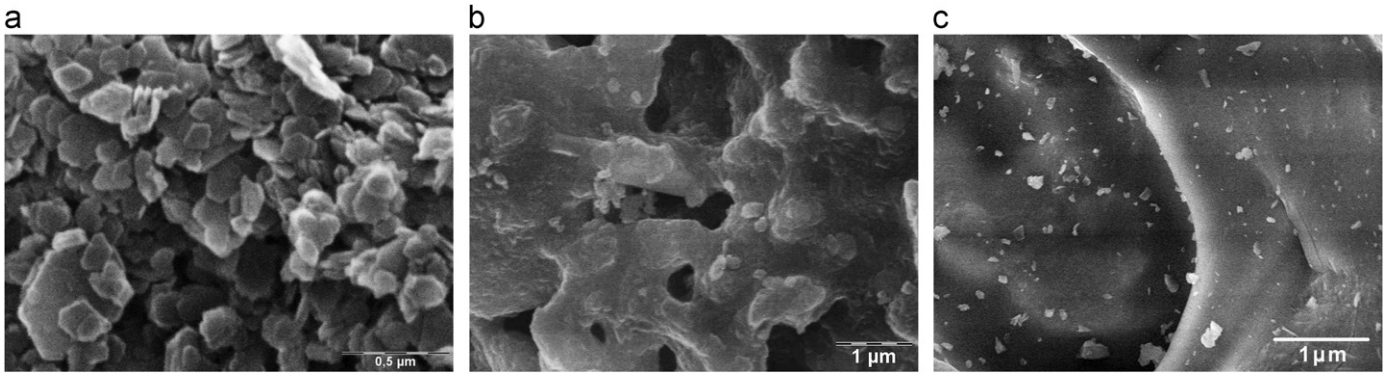

Fig. 4. SEM Photos of the porcelain fired at 1300 °C. (a): raw kaolin; (b): chamotte kaolin at 1300 °C; (c): chamotte porcelain.

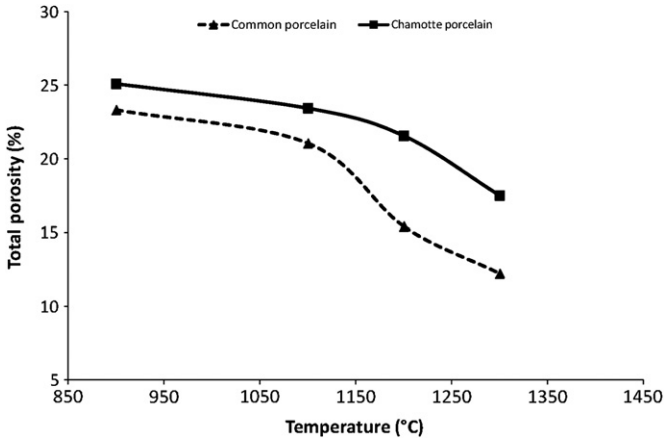

Fig. 5. Porosity of porcelains against temperature.

starting quantity of anatase grains (10 wt%), encapsulated in the heat transformed kaolinite.

The quantitative analysis of the mineralogical phases formed during the sintering of different porcelains is reported in Table 2. The amount of rutile is high in chamotte porcelains. The addition of anatase is accompanied by the increase of cristobalite and mullite and the decrease of the amorphous phase contents.

Porosity measurements as a function of temperature (Fig. 5) show a significant decrease, to achieve 17 vol% and 12 vol% for chamotte and common porcelains respectively. Open porosity is more predominant in Chamotte porcelains than in common porcelain. Open porosity is mostly in the form of very fine pores (Fig. 4a–c), with irregular shapes that are strongly linked [18]. The closed porosity is in the form of large and more spherical isolated pores usually encountered in similar materials [19]. Large closed pores are mostly present in chamotte porcelain than in common porcelain. The glassy matrix is clearly present around grains in chamotte porcelain, but irregularly distributed in common porcelain.

The addition of anatase negatively influences porosity and the amount of amorphous phase. It seems that encapsulation of isolated grains should prevent their interactions, and such phenomenon is significantly increased in chamotte porcelain. The presence of local small cracks should results from distributed TiO_2 grains that locally change the melting and wetting processes of the glassy phase [16].

The completion of the firing process cannot be considered as complete until porosity disappears, since the increase of closed porosity begins before the significant decrease of open porosity [20,21]. This behavior is accompanied with both mullite crystallization and quartz dissolution in the liquid phase. It induces both the increase of liquid phase viscosity and the porosity reduction. The relatively high quantity of Al_2O_3 (at least 25 wt%) induces a more refractoriness behavior during firing at temperature of 1300 °C, which seems to be too low to extensively promote the formation of the glassy phase. The role of the liquid phase in microstructure formation and porosity reduction is not as predominant as in vitrified porcelain [21,22].

The presence of TiO_2 in the form of rutile favors the formation of secondary mullite, mainly in chamotte porcelain. Correspondingly, Hong and Messing [23,24] reported that anatase addition above 5 wt% induces a significant growth of anisotropic mullite crystals at high temperature. It is due to the very limited rutile reaction with mullite, but also causes a significant closed porosity in chamotte porcelain.

The partial dissolution of TiO_2 into the glassy phase occurs as soon as the melting of feldspar grains becomes significant above 1200 °C [25]. This lowers the glassy phase viscosity and modifies the kinetic of the dissolution–recrystallization process of new phases. It also induces the increase of the kinetic of growth of mullite crystals since a dissolution–precipitation process in the liquid predominates at high temperature [26]. The secondary mullite is nucleated at interfaces between the glassy phase and outer surfaces of primary mullite [26].

The relative permittivities of the different samples at a frequency of 100 kHz are relatively high (Table 4). The highest value corresponds to chamotte porcelain ($\varepsilon_r = 8.41$), however common porcelain has a lower value of $\varepsilon_r = 7.19$. It is correlated with rutile dissolution in the glassy phase and probably by the limited substitution of Al^{3+} by Ti^{4+} in octahedral mullite sites that weakly influence the global dielectric properties. Besides, we observe the relatively high dielectric permittivity of common porcelain ($\varepsilon_r = 7.19$) in

comparison to that of manufactured porcelains ($5 < \varepsilon_r < 6$), that evidences the role of relatively high rutile and anatase quantities in KT raw kaolin.

The real part of the complex permittivity $\varepsilon_r = \varepsilon'_r + \varepsilon''_r$ of porcelains at high frequencies of 10^{6-9} Hz reveals a progressive decrease with frequency (Fig. 6). For common porcelain in the higher frequency range of 10^{7-9} Hz, permittivity decrease is limited down to $\varepsilon_r = 5.12$.

The macroscopic value of dielectric properties of porcelains are related to porosity, crystalline and amorphous phase contents, and to the permittivity of the anatase and rutile phases [27]. A mixing rule can be used to calculate the bulk permittivity [27]:

$$\varepsilon_{th} = (X_m \times \varepsilon_m + X_q \times \varepsilon_q + X_C \times \varepsilon_C + X_r \times \varepsilon_r + X_a \times \varepsilon_a + X_g \times \varepsilon_g) \times (1\pi) + \pi \quad (2)$$

where X_m, X_q, X_c, X_r, X_a and X_g are weight percentages of present phases: mullite, quartz, cristobalite, rutile, anatase, and amorphous phase considered as a glass phase. ε_m, ε_q, ε_c, ε_r, ε_r and ε_g are permittivity of each phase and π is the porcelain porosity. Knowing relative permittivity of mullite ($\varepsilon_r = 4$), quartz and cristobalite ($\varepsilon_r = 5.4$), and silicate glass ($\varepsilon_r = 7$), it is possible to calculate the permittivity of the bulk phase, considering the high relative permittivity of rutile $\varepsilon_r = 89$ and that of anatase $\varepsilon_r = 48$ [27].

Porosity can be taken into account by the following relation:

$$\varepsilon_{\exp} = \varepsilon_C \times (1\pi) + \pi \quad (3)$$

where π is porosity (vol%).

In Table 5, we note the significant porosity role in chamotte and common porcelains, considering the large difference between ε_{th} and ε_c. Results also reveal a clear increase of relative permittivity with rutile and anatase contents. It evidences that the rate of anatase to rutile transformation process during firing has a very efficient role in permittivity. In general, a delayed transformation is attained using a high anatase content in initial mixtures of chamotte porcelain, but we note that it is accompanied by the increase of porosity.

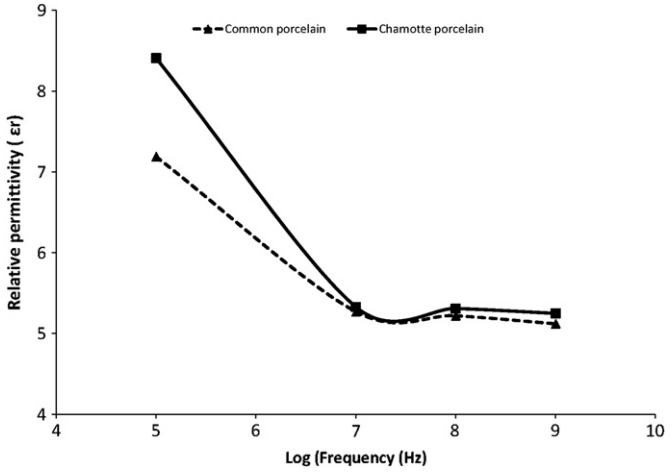

Fig. 6. Variation of relative permittivity versus frequency of porcelains.

The increased permittivity is obtained by the natural encapsulation of anatase nanocrystals within phyllosilicate layers in KT kaolin. During chamotte firing and the subsequent chamotte porcelain firing, anatase nanocrystals are encapsulated by the phyllosilicate matrix phase. In a similar situation, the transformation mechanism of anatase was studied with 100 nm TiO_2 powders, during heat-treatment [15]. Authors evidenced specific orientation relationship between anatase and rutile. Grain growth of the rutile transformed phase was observed by a coarsening mechanism involving interactions with neighboring initial anatase, and also requires specific crystallographic orientations. In the case of anatase nanocrystals within phyllosilicate layers, which size (~200 nm; Table 3) is close to that studied by Gouma and Mills [15], this induces the reduction of the rutile to anatase transformation rate and limits the coarsening of nanocrystals by grain aggregation. Whereas the small anatase content, it is sufficient to obtain a significant increase of the macroscopic permittivity.

The encapsulation of anatase and rutile is illustrated in SEM photos. In Fig. 4a, the crystal size of kaolinite is in the range 0.2–0.5 m. The well crystallized and flat shape of kaolinite favors the dispersion of sub-micron anatase crystals, which average sizes are in Table 3. After heating at 1300 °C, kaolinite platelets form densified zones, where relicts of crystallite shape are seen. Dense zones are able to encapsulate isolated sub-micron rutile and anatase crystals. The microstructure of chamotte porcelain at the interface of matrix and chamotte phases (Fig. 4c) shows the limited interaction between the glassy phase of porcelain and chamotte grains. It evidences that anatase and rutile crystals in chamotte are far from the liquid phase interaction at high temperature.

Dielectric loss of porcelains in the frequency range of 10^5–10^9 Hz is shown in Table 6. They are larger at low frequencies than at high frequency. Chamotte porcelain has larger dielectric loss, which is probably due to the role of TiO_2 nanocrystals, which exhibit a significant relaxation process in the 10^5–10^6 Hz interval [12]. For common porcelain, the dielectric loss is weaker since the concentration, size distribution and shape of the crystalline phases in glassy matrix influence the losses and dielectric constants [17].

5. Conclusion

At 1300 °C, anatase mineral from the starting kaolin (KT) is not completely transformed into rutile. It induces a significant increased of the relative permittivity of porcelain containing KT kaolin. In a similar way, the addition of anatase in the porcelains mixture also induces the increase of permittivity, and it is accompanied by the increase of porosity.

The addition of 10 wt% of anatase in porcelain results in a higher porosity and the delayed formation of the glassy phase that induce microstructural heterogeneities. Porcelain containing pre-fired (1300 °C) kaolin–anatase mixture present better dielectric properties in comparison with that of

common porcelain. It is due to the low anatase to rutile transformation rate of nanocrystals within phyllosilicate layers. In that case a small content of nanometric TiO_2 crystals is sufficient to favor a significant increase of permittivity. In comparison, common porcelain presents a more homogenous microstructure and a lower porosity, but a low permittivity, which can be increased by the addition of kaolin containing anatase mineral.

References

[1] M. Dondi, C. Iglesias, E. Dominguez, G. Guarini, M. Raimondo, The effect of kaolin properties on their bahaviour in ceramic processing as illustrated by a range of kaolins from the Santa Cruz and Chubut Provinces, Patagonia (Argentina), Applied Clay Science 40 (2008) 143–158.

[2] M. Felhi, A. Tlili, M.E. Gaied, M. Montacer, Mineralogical study of kaolinitic clays from Sidi El Bader in the far north of Tunisia, Applied Clay Science 39 (2008) 208–217.

[3] R.N. Maynard, N. Millman, J. Iannicelli, J.M. Huber, A method for removing titanium dioxide impurities from kaolin, Clays and Clay Minerals 17 (1969) 59–62.

[4] F. Belnou, D. Goeuriot, P. Goeuriot, F. Valdivieso, Nanosized alumina from boehmite additions in alumina porcelain. Part 2: Effect on material properties, Ceramics International 33 (2007) 1243–1249.

[5] S.P. Chaudhuri, P. Sarkar, Constitution of porcelain before and after heat treatment, I: Mineralogical composition, Journal of the European Ceramics Society 15 (1995) 1031–1035.

[6] A.J. Moulson, J.M. Herbert, Electroceramics: Materials, Properties, Aapplications, second ed., John Wiley and Sons, United States, 2003.

[7] L.A. Harris, A titanium dioxide hydrogen sonsor, Journal of the Electrochemical Society of Solid State Sciences and Technology 127 (1980) 2657.

[8] B.H. Park, L.S. Li, B.J. Gibbons, J.Y. Huang, Q.X. Jia, Photovoltaic response and dielectric properties of epitaxial anatase–TiO_2 films grown on conductive $La_{0.5}Sr_{0.5}CoO_3$ electrodes, Applied Physics Letters 79 (2001) 2797–2800.

[9] F.A. Grant, Properties of rutile (titanium dioxide), Reviews of Modern Physics 31 (1959) 646–674.

[10] Jin Young Kim, Hyun.Suk Jung, Jung.Hong No, Jeong-Ryeol Kim, Kug.Sun Hong, Influence of anatase–rutile phase transformation on dielectric properties of sol–gel derived TiO_2 thin films, Journal of Electroceramics 16 (2006) 447–451.

[11] C.T. Dervosa, Ef. Thiriosa, J. Novacovicha, P. Vassilioub, P.Skafidas, Permittivity properties of thermally treated TiO2, Materials Letters 58 (2004) 1502–1507.

[12] L.D. Zhang, H.F. Zhang, G.Z. Wang, C.M. Mo, Y. Zhang, Dielectric behavior of nano-TiO_2 bulks, Physics Status Solidi A 157 (1996) 483–491.

[13] M. Horn, C.F. Schwerdtfeger, E.P. Meagher, Refinement of the structure of anatase at several temperatures, Zeitschrift Für Kristallographie 136 (1972) 273–281.

[14] R.D. Shannon, J.A. Pask, Kinetics of the anatase–rutile transformation, Journal of the American Ceramics Society 48 (1965) 391–398.

[15] P.I. Gouma, J.M. Mills, Anatase-to-rutile transformation in titania powders, Journal of the American Ceramic Society 84 (2001) 619–622.

[16] W.M. Carty, U. Senapati, Porcelain-raw materials, processing, phase evolution and mechanical behavior, Journal of the American Ceramic Society 81 (1998) 3–20.

[17] S.P. Chaudhuri, P. Sarkar, Dielectric behaviour of porcelain in relation to constitution, Ceramics International 26 (2000) 865–875.

[18] T. kalecec, E. Prodanovic, D. Falz, H.W. Hennicke, Microstructure and properties of aluminous electrical porcelain doped with $BaCO_3$, Transactions of the British Ceramics Society 84 (1985) 94–98.

[19] J.M. Márquez, J.M. Rincón, M. Romero, Effect of firing temperature on sintering of porcelain stoneware tiles, Ceramics International 34 (2008) 1867–1873.

[20] W.E. Lee., W.M. Rainforth, Ceramic Microstructures: Property Control by Processing, Chapman and Hall, UK, 1995.

[21] A.W. Norris, D. Taylor, I. Thorpe, Range curves: an experimental method for the study of vitreous pottery bodies, Transactions of the British Ceramic Society. 78 (1979) 102–108.

[22] S. Maity, B.K. Sarkar, Development of high-strength whiteware bodies, Journal of the European Ceramic Society 16 (1996) 1083–1088.

[23] S.H. Hong, G.L. Messing, Mullite transformation kinetics in P_{205}-, TiO_2-, and B_{203}- doped alumino sillicate gels, Journal of the American Ceramic Society 80 (1997) 1551–1559.

[24] S.H. Hong, G.L. Messing, Anisotropic grain growth in diphasic-gel-derived titania doped mullite, Journal of the American Ceramic Society 81 (1998) 1269–1277.

[25] N. Montoya, F.J. Serrano, M.M. Reventós, J.M. Amigo, J. Alarcón, Effect of TiO_2 on the mullite formation and mechanical properties of alumina porcelain, Journal of the European Ceramic Society 30 (2010) 839–846.

[26] D.R. Stewart, TiO_2 and ZrO_2 as nucleants in a lithia aluminosilicate glass–ceramics, in: L.L. Hench, S.W. Freiman (Eds.), Advances in Nucleating and Cristallization in Glasses, American Ceramic Society, Clombus, 1971, pp. 83–90.

[27] S.P. Chaudhuri, P. Sarkar, Dielectric behavior of porcelain in relation to constitution, Ceramics International 26 (2000) 865–875.